Nuclear Engineering and Technology 51 (2019) 1749–1757

Contents lists available at ScienceDirect

Nuclear Engineering and Technology

journal homepage: www.elsevier.com/locate/net

Original Article

A flammability limit model for hydrogen-air-diluent mixtures based on heat transfer characteristics in flame propagation

Joongoo Jeon [a], Wonjun Choi [a], Sung Joong Kim [a, b, *]

[a] Department of Nuclear Engineering, Hanyang University, 222 Wangsimni-ro, Seongdong-gu, Seoul 04763, Republic of Korea
[b] Institute of Nano Science & Technology, Hanyang University, 222 Wangsimni-ro, Seongdong-gu, Seoul, 04763, Republic of Korea

ARTICLE INFO

Article history:
Received 2 January 2019
Received in revised form
15 March 2019
Accepted 2 May 2019
Available online 3 May 2019

Keywords:
Hydrogen combustion
Lower flammability limit
Radiative heat transfer
CAFT
CNAFT
Severe accident

ABSTRACT

Predicting lower flammability limits (LFL) of hydrogen has become an ever-important task for safety of nuclear industry. While numerous experimental studies have been conducted, LFL results applicable for the harsh environment are still lack of information. Our aim is to develop a calculated non-adiabatic flame temperature (CNAFT) model to better predict LFL of hydrogen mixtures in nuclear power plant. The developed model is unique for incorporating radiative heat loss during flame propagation using the CNAFT coefficient derived through previous studies of flame propagation. Our new model is more consistent with the experimental results for various mixtures compared to the previous model, which relied on calculated adiabatic flame temperature (CAFT) to predict the LFL without any consideration of heat loss. Limitation of the previous model could be explained clearly based on the CNAFT coefficient magnitude. The prediction accuracy for hydrogen mixtures at elevated initial temperatures and high helium content was improved substantially. The model reliability was confirmed for H_2-air mixtures up to 300 °C and H_2-air-He mixtures up to 50 vol % helium concentration. Therefore, the CNAFT model developed based on radiation heat loss is expected as the practical method for predicting LFL in hydrogen risk analysis.

1. Introduction

The catastrophic experience of the Fukushima accident in 2011 underlines the importance of research activities over the risks of hydrogen combustion under severe accidents [1]. It is because hydrogen explosion can impose dynamic mechanical and thermal loads to the containment building [2,3]. To cope with the raised standard over the safety of nuclear power plant, hydrogen combustion and its flammability limit are recognized as critical topics to the worldwide nuclear society [4,5]. A new approach was also taken by Kim et al. to predict hydrogen concentration in containment during severe accidents using fuzzy neural network [6]. More specifically, Yu et al. and Malik et al. suggested the machine learning model to predict the detonation cell width which is an important parameter in hydrogen explosion assessments [7,8]. As such, systematic efforts to improve the understanding of the hydrogen combustion and its risk are essential for guaranteeing the safety of nuclear power plant. A part of the systematic effort may be credited to the overall assessment of the nuclear power plant using severe accident codes such as MELCOR and MAAP. However, these codes adopt a rather simple logic for predicting the lower flammability limit (LFL). The LFL is the minimum concentration of flammable gas which can continuously propagate flame. If the hydrogen concentration in the containment exceeds the LFL, a more detailed risk analysis of the NPP should be performed to verify the potential risk of flame acceleration (FA) and detonation [3]. For example, the MELCOR code uses a constant LFL of 4.1 vol% regardless of the mixture conditions [9]. This simple constant logic can significantly increase the uncertainty of severe accident hydrogen risk analysis because this threshold concentration largely depends on the mixture conditions, such as initial temperature and diluent concentration. Thus, thorough understanding of the LFL of hydrogen can contribute to improving accuracy of nuclear safety analysis. Nikolaidis et al. noted that the understanding of the flammability range is also extensively required for transportation and utilization of hydrogen fuel [10].

Abbreviation: CAFT, Calculated adiabatic flame temperature; CNAFT, Calculated non-adiabatic flame temperature; FA, Flame acceleration; LFL, Lower flammability limit; UFL, Upper flammability limit; NPP, Nuclear power plant.

* Corresponding author. Department of Nuclear Engineering, Hanyang University, 222 Wangsimni-ro, Seongdong-gu, Seoul 04763, Republic of Korea.
E-mail address: sungjkim@hanyang.ac.kr (S.J. Kim).

https://doi.org/10.1016/j.net.2019.05.005

Nomenclature

C	Molar concentration (mol/m^3)
c_p	Heat capacity at constant pressure (J/kg K)
D	Diameter (m)
E_a	Activation energy (J/mol)
ΔH_f^0	Standard formation enthalpy (J/mol)
H^a	Energy released per unit mass of the mixture (J/kg)
h	Heat transfer coefficient (W/m^2·K)
k	Thermal conductivity (W/m K)
$\Delta T/L$	Local temperature gradient at the flame front (K/m)
n	Number of moles (mole)
Q_{loss}	Volumetric heat loss (kJ/mol)
q_{loss}	Heat loss per unit area (W/m^2)
q_{conv}	Convective heat loss per unit area (W/m^2)
q_{rad}	Radiative heat loss per unit area (W/m^2)
R	Gas constant (8.314 J/mol K)
R_r	Space averaged radiative volumetric heat loss (W/m^3)
$R(T)$	Radiative volumetric heat loss (W/m^3)
S_u	Laminar flame speed (m/s)
T_f	Peak flame temperature (K)
T_u	Unburnt mixture temperature (K)
T_{ref}	Reference temperature (K)
T_{CAFT}	Calculated adiabatic flame temperature (K)
T_{CNAFT}	Calculated non-adiabatic flame temperature (K)
$\dot{w}$	Reaction rate (kg/m^3·s)

Greek letters

ρ_u	Unburnt mixture density (kg/m^3)
δ	Flame thickness (m)
α	Thermal diffusivity (m^2/s)
π	CNAFT coefficient

Because the knowledge concerning the LFL is also required for hydrogen industry, the flammability limits of hydrogen mixtures have been investigated through many experimental studies. Regardless of the extensive experimental results, there is a lack of information for identifying the limits for all possible mixture conditions. In particular, the observations for mixtures with the presence of diluents and the elevated temperature corresponding to the severe accident conditions is insufficient as shown in Fig. 1. For this reason, it is imperative to develop a theoretical model to accurately predict the LFL in contingency with mixture conditions [11]. Recently, significant efforts to the LFL were focused on the details of multi-step chemical kinetic mechanisms, which significantly limited the utility of their method. These are a great asset for the hydrogen risk study. However, a special attention needs to be paid to the extinction condition, which lost the generality of a thermal system when computing the involved chemistry [12].

Many historical attempts also have been made to explain the flammability limit via thermal theories. Explanation of the limit by heat loss mechanism for the radiative heat loss through the walls of the combustion chamber was attempted by Spalding [13]. Recently, Vidal et al. pointed out that calculated adiabatic flame temperature (CAFT) is a powerful model for estimating the LFL of gaseous mixtures [14]. It was found in many studies that the CAFT remains nearly constant regardless of the properties of the limiting

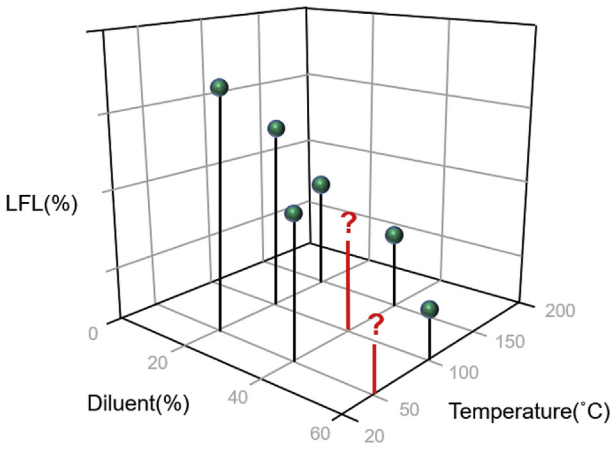

Fig. 1. The need for a universal LFL model that can simultaneously consider the diluent concentration and temperature changes.

mixtures. These studies remarked that the threshold peak temperature for flame propagation was proportional to the CAFT [15–17]. More recently, Shu et al. proved that CAFT model is also effective for evaluating the flammable regions of hydrocarbon-air-CO_2 mixtures and Wu et al. identified that a model based on adiabatic flame temperature can precisely predict the upper flammability limit (UFL) for various fuel mixtures [18,19]. However, researchers have found that relying on the CAFT concept tends to result in inconsistent accuracy results depending on the mixture conditions. This is especially true when the initial temperature of mixture is high or the diluent gas is helium. The limitations of the CAFT model came from its dependence on an adiabatic value whereas actual flame propagation involves heat loss mechanisms. The amount of heat loss substantially affects the peak flame temperature and hence determines the intrinsic LFL value of the mixture [12,13,20].

Therefore, our aim is to develop a calculated non-adiabatic flame temperature (CNAFT) model to predict the LFL at elevated temperatures and additional diluents. The proposed model analyzes the flame physics in a non-adiabatic condition based on studies of heat loss mechanisms during upward propagation. The reason why the CAFT model showed poor accuracy for mixtures under high initial temperatures or in the presence of helium was expected to be explained by these heat loss mechanisms. The heat loss estimation methodology through CNAFT coefficient was verified through Terpstra's flammability experiments based on atmospheric pressure [21]. Finally, the reliability of the CNAFT model was identified by the experimental results obtained by various researches [21–23]. In addition, the mixtures that initially contain steam will be investigated in our future study because of characteristics of radiating species.

2. Limitation of the calculated adiabatic flame temperature

According to Arrhenius theory, the peak temperature T_f occurring at the flame front determines the chemical reaction rate $\dot{w}$ as shown in Equation (1), where E_a is the activation energy and R is the ideal gas constant [24]. When the peak temperature rises, the number of molecules participating in the reaction increases. The threshold peak temperature is the temperature that can produce the minimum reaction rate to sustain propagation [15–17]. Previous studies concluded that the threshold peak temperature being determined by fuel type was proportional to the CAFT of the limiting mixtures [14]. Because direct prediction of the peak

temperature is almost impossible, for LFL prediction, the peak temperature has been estimated by the CAFT. The CAFT can be calculated from the energy conservation equation with adiabatic condition as shown in Equation (2), where n_i is the number of molecules and $\Delta H^0_{f,i}$ is the formation enthalpy of species i and T_{ref} is the reference temperature, 298 K. The average heat capacity $\bar{c}^0_{p,i}$ was calculated for each compound using the corresponding adiabatic flame temperature.

$$\dot{w} \sim \exp\left(-E_a/RT_f\right) \tag{1}$$

$$\sum n_i\left[\Delta H^0_{f,i}\right]_{reactants} - \sum n_i\left[\Delta H^0_{f,i} + \bar{c}_{p,i}\left(T_{CAFT} - T_{ref}\right)\right]_{products} = 0 \tag{2}$$

However, the limitations of this concept were confirmed through experimental results. Terpstra experimentally determined the flammability limits of various hydrogen-diluent fuel mixtures in the air for upward propagation at ambient pressure [21]. In these experiments, they used a tube of 51 mm in diameter and 1 m in length, which was similar to that used by the US Bureau of Mines [25]. These dimensions allowed the experimenters to observe the widest flammability limits that would propagate on their own in the air while reducing the influence of the ignition source. Kumar and Hustad also experimentally observed the limits of hydrogen mixtures for upward propagation using the vertical chamber [22,23]. Table 1 shows these experimental LFL results of each hydrogen mixture including the value of CAFT based on the determined limiting mixtures. Although the temperature remains nearly constant for various mixtures at approximately 600 K, other mixtures show significant differences. Some mixtures even have the temperature of 800 K. This finding is the most pronounced when the initial temperature is high or the helium gas is included. This discrepancy is more noticeable in the comparison between the predicted LFL and the experimental results as shown in Fig. 2. As a result, it was confirmed that the model showed inconsistent accuracy depending on the mixture conditions. This limitation could be due to the simplified assumption of adiabatic flame expansion. In reality, however, flames do not propagate under adiabatic conditions, and heat loss processes play a part. It means that the effects of heat loss depending on the mixture conditions should be considered when predicting the LFL.

Table 1
CAFT for various limiting mixtures [21–23].

Researcher	Mixture	T_i (°C)	Diluent (vol%)	LFL (vol%)	CAFT (K)
Terpstra	H_2-air	20	0	3.9	610
	H_2-air	50	0	3.8	633
	H_2-air	100	0	3.6	667
	H_2-air	150	0	3.3	692
	H_2-air	200	0	2.8	701
	H_2-air	300	0	2.4	769
	H_2-air-He	20	0–50	3.8–5.3	600-800
	H_2-air-Ar	20	0–60	3.0–3.8	590-610
	H_2-air-N_2	20	0–20	~3.9	~610
Kumar	H_2–O_2–He	22	20–40	5.1–5.8	700–800
	H_2–O_2–He	100	20–40	3.9–4.3	700-750
	H_2–O_2–N_2	22	20–40	~4.0	~600
	H_2–O_2–N_2	100	20–40	~3.5	~650
Hustad	H_2-air	20	0	4.3	644
	H_2-air	200	0	3.3	741

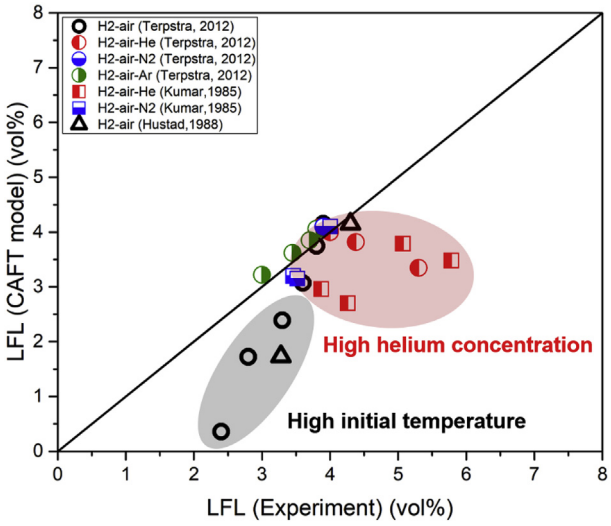

Fig. 2. Validation of CAFT model for various mixtures in Table 1. Two representative groups with large discrepancy.

3. Development of a calculated non-adiabatic flame temperature model

3.1. Heat loss mechanism during flame propagation

The effects of the heat loss from the reaction zone to the post-reaction zone play a significant role in determining the peak temperature. It means that the heat loss mechanism ultimately affects the intrinsic flammability limit of gas mixtures [12,13,20]. If there is no heat loss during flame propagation, all the combustion heat can be transferred to the unburned gas. In this case, the peak flame temperature can be sustained once heat above the activation energy is supplied. On the other hand, if the heat loss to the post-reaction zone is considered, the peak temperature assumed to occur near the end of the reaction zone can be calculated using an energy balance equation as shown in Equation (3). ρ_u is the unburnt mixture density, c_p is the isobaric specific heat capacity, H^a is the energy released per unit mass of the mixture, T_u is the temperature of unburnt mixture, q_{loss} is the heat loss rate per unit area of the flame front, and S_u is the actual flame speed. The essential heat loss mechanisms considered when applying Equation (3) for the prediction of flammability limits are the convective and radiative heat transfer from the flame to the environment [26,27]. In this study, the effect of a specific flame structure depending on mixture conditions was not considered because the combustion regime of the observed cap-like flames at the ultra-lean H_2-air mixture is not fully understood [28]. Especially, the identification of flame regimes in condition of diluents is still lacking. Although the approach with the one-dimensional energy equation is difficult to depict local heat transfer phenomena, it makes possible to estimate sum of heat loss in the reaction zone. Therefore, the convective heat loss can be calculated as the heat loss rate per unit area of the flame as shown in Equation (4). In this equation, h is heat transfer coefficient, T_u is the tube wall temperature which is assumed to be equal to the unburnt mixture temperature, and $\pi D\delta$ is the heat transfer area.

$$\rho_u S_u\left[c_p T_u + H^a\right] - \rho_u S_u c_p T_f - q_{loss} = 0 \tag{3}$$

$$q_{conv} = \frac{h\left(T_f - T_u\right)\pi D\delta}{\pi D^2/4} \tag{4}$$

However, convective heat loss can be ignored if the tube diameter is larger than a certain value. Fernandez-Galisteo explained that the convection can be neglected in the reaction zone because the burnt temperature is close to crossover value for lean flames close to the flammability limit [29]. This approach has been applied for a standard apparatus for determining the flammability limits, as done by Coward and Jones. Such apparatus consisted of a vertical tube 51 mm in diameter and 1.8 m long, closed at the upper end and open to the atmosphere at the bottom [25]. The flame propagation in this corresponding geometry is the subject of our study. Therefore, the radiative heat loss was considered dominant in the energy balance of the flame front [20].

3.2. Implementation of radiative heat loss

The effects of radiative heat loss from the flame to the ambient environment can be classified as conduction of heat into the post-reaction zone, which is cooled via radiative heat loss $q_{rad,1}$ and radiative heat loss from the reaction zone itself, $q_{rad,2}$ as shown in Fig. 3 [27]. First, the heat conduction into the post-reaction zone is caused by the temperature gradient near the end of the reaction zone. In one-dimensional and steady-state flame propagation, the temperature distribution in the post-reaction zone can be calculated in Equation (5). $R(T)$ is the radiative volumetric heat loss rate dependent on the local temperature distribution and the mixture properties. Through a scaling analysis, it can be deduced that the transport term on the left of Equation (5) is much greater than the diffusion term, as shown in Equation (6). $\Delta T/L$ is the local temperature gradient at the flame front. Therefore, near the end of reaction zone, a peak temperature gradient under the influence of radiative heat losses can be solved through Equation (7). Mayer also noted that this approximation using scaling analysis is possible over the range of mass flow rates in typical flame propagation [27].

$$\rho_u c_p S_u \frac{dT}{dx} - \frac{d}{dx} k \frac{dT}{dx} = -R(T) \tag{5}$$

$$\frac{\rho_u c_p S_u \Delta T}{L} \gg \frac{k \Delta T}{L^2} \tag{6}$$

$$\left(\frac{dT}{dx}\right)_{x=x_f} = -\frac{R\left(T_f\right)}{\rho_u c_p S_u\left(T_f\right)} \tag{7}$$

Finally, the heat loss rate from the reaction zone due to the conduction into the post-reaction zone can be estimated using Equation (8). The unit area is based on the flame front. The equation includes several variables determined by the mixture properties. The thermal conductivity value used is the one at the flame front, while the density and specific heat are those of the unburned gas.

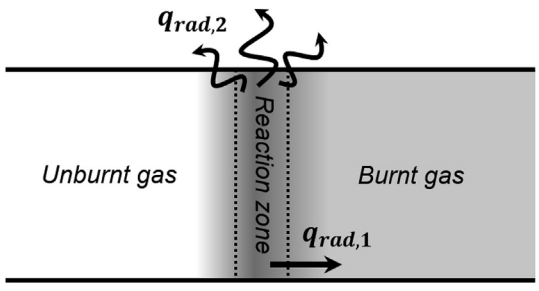

Fig. 3. Two kinds of radiative heat loss mechanisms during flame propagation.

$$q_{rad,1} = -k_f \left(\frac{dT}{dx}\right)_{x=x_f} = k_f \frac{R\left(T_f\right)}{\rho_u c_p S_u\left(T_f\right)} \tag{8}$$

Second, the radiative heat loss rate from the reaction zone itself is calculated via integration, as shown in Equation (9). However, Mayer announced that $q_{rad,2}$ can be ignored inasmuch as the space-average value of R_r in the reaction zone is much lower than $R(T_f)$ [27]. It is very difficult to calculate the precise amount of $q_{rad,2}$ because accurate analysis of local radiative heat transfer during flame propagation is required. Recently, Liaw et al. investigated the effect of $q_{rad,2}$ on LFL prediction based on the concept of maximum value. As a result, the LFL prediction value for various hydrogen mixtures varied about 0.2 vol% on the average [30]. This variation is considered negligible given that the current CAFT model exhibits an error of more than 2 vol.% compared with the experimental results. Lakshmisha et al. also proved that the fraction of $q_{rad,2}$ was very small compared to heat release rate for CH_4-air. They numerically solved the equations for premixed flames near lean flammability limits, considering detailed chemistry and variable properties [31].

$$q_{rad,2} = \int_0^{\delta} R_r dx \tag{9}$$

These conclusions are also consistent with the experimental observations of Shoshin et al. that limit flame extinction behavior is connected with the formation of the stagnation zone of combustion products. They pointed out that the reaction zone is effectively cooled by heat conduction to the stagnation zone, which rises upward together with flame and cooled due to radiation heat loss [32]. As a result, most of the heat loss determining the peak temperature can be estimated only by regarding the conduction of heat into the post-reaction zone, which is cooled via radiative heat loss $q_{rad,1}$.

3.3. Construction of a calculated non-adiabatic flame temperature model

As shown in Equation (10), the magnitude of the radiative heat loss rate can be determined using the thermal diffusivity, flame speed, and volumetric heat loss rate. In ultra-lean H_2-air flames, the laminar flame speed is severely affected by cellular instabilities as the stretch rate approaches zero. This is the profound characteristic for unstretched flames that the Lewis number is much smaller than one [33]. The flame speed of the limiting mixtures is independent of the mixture properties and its finite value can be calculated from the results presented by Davies and Taylor [34]. Their observations were derived from experimental results, which proved that an upward propagating flame at the limit of flammability has properties in common with a rising Taylor bubble of hot gas [35]. On the other hand, according to a previously proposed optically thin radiation model, volumetric heat loss rate is determined by the threshold peak temperature and the presence of radiating species [20]. Because the threshold peak temperatures of the limiting mixtures were assumed to be invariable, the volumetric heat loss rate was considered to be constant with the exception of mixtures containing the radiating species. Consequently, it was experimentally and theoretically suggested that radiative heat loss rate $q_{rad,1}$ can be determined using a linear function of thermal diffusivity. Mixtures that initially contain steam classified as the radiating species will be investigated in the further study.

Henceforth we determined that the amount of heat loss rate

during flame propagation can be estimated through the radiative heat loss rate $q_{rad,1}$. Therefore, in this study, Equation (2) was modified into Equation (11) to build an LFL prediction model by considering radiative heat transfer. Thermal diffusivity α is divided by the molar concentration C to predict heat loss in mole units. This equation assumes combustion in a non-adiabatic condition while considering heat loss due to radiative heat transfer. This parameter was defined as a CNAFT coefficient, π, which can be calculated as an average value considering the fraction of each gas component of the mixture. To confirm that the derived coefficient is dominant parameter in heat loss estimation, we divided hydrogen mixtures in Table 1 into two groups and compare the trend with the CAFT model. First group includes the mixtures having lower CNAFT coefficient than the ambient air. The initial temperature of all these mixtures is less than 100 °C. Second group has the higher CNAFT coefficient than the ambient air. Since the helium gas has a large coefficient value, the mixture containing helium gas are classified in the second group even at room temperature. The fundamental reason for the large coefficient value of helium gas is its high thermal conductivity. The quantitative effects of the thermal properties on the coefficient were discussed in detail later. Fig. 4 shows the average relative error of the predicted LFL value for each type of hydrogen mixture. It is noted that the accuracy of CAFT model was completely different depending on the group. While the all of mixture in first group has the relative error less than 6%, the second group have the maximum relative error close to 40%. These results suggested that the CNAFT coefficient, which can estimate the heat loss amount, can clearly explains the limitation of CAFT model.

$$q_{rad,1} = k_f \frac{R(T_f)}{\rho_u c_p S_u(T_f)} = \frac{R(T_f)}{S_u(T_f)} \alpha \sim \alpha \tag{10}$$

$$\sum n_i \left[\Delta H^0_{f,i}\right]_{reactants}$$

$$-\sum n_i \left[\Delta H^0_{f,i} + \bar{c}_{p,i}\left(T_{CNAFT} - T_{ref}\right)\right]_{products} = Q_{rad,1} \sim \alpha / C \tag{11}$$

The mechanistically derived linearity in Equation (10) as well as the suitability of the coefficient was validated using the experimental results by Terpstra in Table 1 [20]. To validate this linear relationship, a reference mixture was required for calculating relative amount of heat loss. The reference mixture was selected to be the H_2-air mixture at 20 °C. It is because the heat loss effects on LFL significantly changes from the CNAFT coefficient on the ambient air condition. The LFL prediction in the adiabatic condition does not produce a noticeable error until the coefficient value at the reference mixture. Thus, the difference in heat loss for each mixture was inversely estimated using Equation (11) based on 610 K, which is value of CAFT at the reference mixture. The difference in CNAFT coefficient was also calculated based on the reference mixture. The thermal conductivity used for calculating the coefficient was substituted with a corresponding value at this temperature. Although the CNAFT cannot directly indicate the peak temperature at the flame front, the gas thermal conductivity is linearly proportional to temperature. It implies that the linear approximation of heat loss is valid if the value of CNAFT remains constant with the threshold peak temperature regardless of the hydrogen mixture type. Fig. 5 shows the difference in volumetric heat loss for each mixture based on their initial mole number before the reaction.

A linear relationship between the two variables predicted by mechanistical analysis was confirmed as shown in Equation (12), which indicates that both variables have a strong linear relationship. The proportional constant was analyzed to be 0.207 with R-square value of 0.98. As mentioned, the constant was expected to the value independent of limiting mixture conditions. Additionally, it should be noted that the mixtures at elevated temperatures and with a high helium concentration have higher CNAFT coefficients than the other mixtures presented in Table 1. When temperature rises, the coefficient increases regardless of the composition of the mixture. In addition, helium gas has its own high CNAFT coefficient due to the mixture properties. These two types of mixtures had in common that predicting the LFL is difficult with the CAFT model. In other words, a mixture having a high coefficient requires more combustion heat to compensate for its higher radiative heat loss than other mixtures. Given that the heat generated by combustion of a lean limit H_2-air mixture at room temperature is about 10 kJ/mol, this difference in the amount of heat loss must be considered.

$$Q_{rad,1}(\pi) = 0.207(\pi - \pi_{air,20°C}),\ \pi = \frac{\alpha}{C}\left[10^3 \cdot \frac{cm^5}{mol \cdot sec}\right] \tag{12}$$

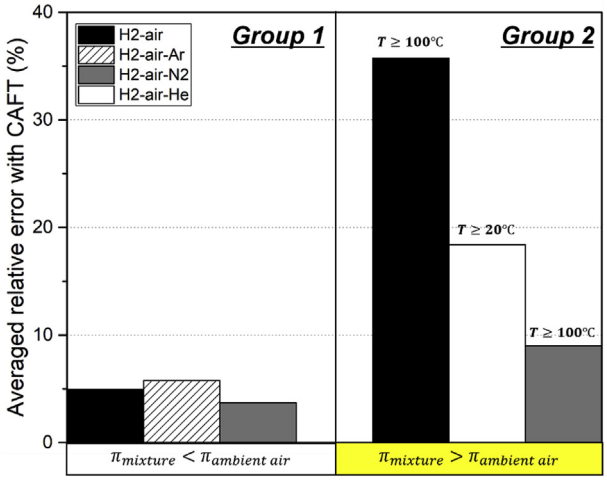

Fig. 4. Classification of mixtures according to CNAFT coefficient to confirm the deterministic effects on heat loss mechanism.

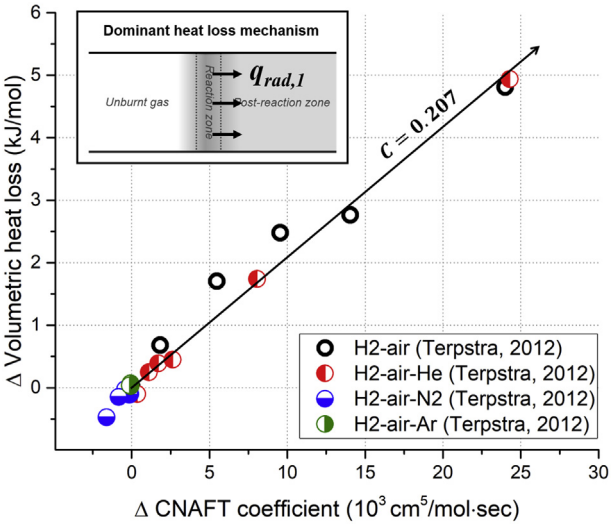

Fig. 5. Linear relationship between the CNAFT coefficient and amount of heat loss. Differences were calculated based on the reference mixture (H_2-air at room temperature).

In conclusion, the CNAFT coefficient can be used to estimate radiative heat transfer based on mixture properties. Variables such as initial temperature, diluent type, and diluent composition ratio affect these mixture properties. By knowing the thermal diffusivity of a mixture for which the LFL is not known experimentally, the amount of heat loss in the CNAFT model can be estimated. Finally, the hydrogen concentration, where the CNAFT reaches 610 K considering the estimated heat loss is the LFL value predicted by the CNAFT model as shown in Equation (13). Fig. 6 shows an example of determining the LFL of an H_2-air mixture at 373 K.

$$\sum n_i\left[\Delta H_{f,i}^0\right]_{reactants} - \sum n_i\left[\Delta H_{f,i}^0 + \bar{c}_{p,i}\left(T_{CNAFT} - T_{ref}\right)\right]_{products} = 0.207\left(\pi - \pi_{air,20^\circ C}\right) \quad (13)$$

4. Results and discussions

4.1. Validation of calculated non-adiabatic flame temperature model

The accuracy of the CNAFT model was validated with the experimental results in Table 1. To identify the model generality, not only Terpstra's data which determined the proportional constant but also Kumar's and Hustad's data were included in the results. The mixtures containing helium and nitrogen at high temperature was investigated in the Kumar's experiment unlike the Terpstra's experiment. As shown in Fig. 7, the reliability of CNAFT model was confirmed for H_2-air mixture up to 300 °C and H_2-air-He mixtures up to 50 vol % helium concentration. It is noted that the maximum relative error is about 13% even for the mixtures, which are difficult to be evaluated using the CAFT model. As mentioned, that representative conditions are elevated temperature and high helium concentration.

First, as the initial temperature increases, the CNAFT coefficient of the mixtures becomes larger. This implies that the amount of heat loss generated during flame propagation also increases with temperature. Thus, the reliability of the CAFT model, which cannot account for the amount of radiative heat loss during continuous flame propagation, dramatically decreases. Because of this, the LFL

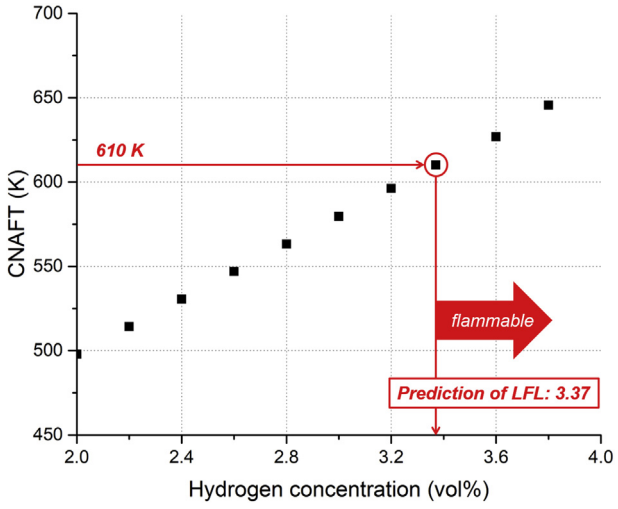

Fig. 6. Determination of LFL in an H_2-air mixture (373 K). The CNAFT model predict the LFL to be 3.37 vol% (Experimental results: 3.6 vol%).

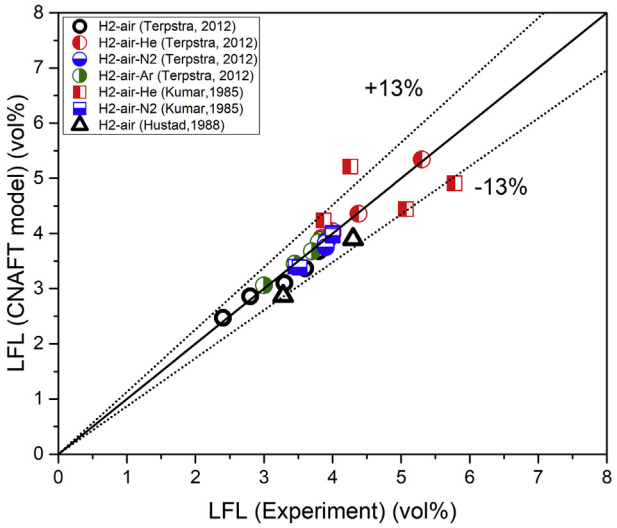

Fig. 7. Validation of CNAFT model for various mixtures. The maximum relative error was analyzed as 13%.

differences between the predicted values and experimental results increases up to 2.0 vol %. In contrast, the CNAFT model reflects the magnitude of radiative heat loss. Therefore, the CNAFT model shows a maximum LFL difference of only 0.5 vol % compared to experimental results for H_2-air mixtures up to 300 °C.

Likewise, as the helium composition increases, the LFL in the experiment increases. Because the CNAFT coefficient of helium is much higher than that of air, the average thermal diffusivity of the mixture increases regardless of the initial temperature. Only the CNAFT model reflects the increase of radiative heat loss according to the helium concentration and exhibits reliable accuracy in comparison with experimental results. The model also shows a maximum LFL difference of only 0.3 vol % compared to experimental results for H_2-air-He mixtures up to 50 vol % helium concentration at room temperature while the CAFT model shows a maximum difference of 2.0 vol %. If the initial temperature of H_2-air-He mixture increases by 100 °C, the maximum difference by CNAFT model slightly increases to 0.5 vol % except for a mixture. In conclusion, this heat transfer-based approach can be applicable to a wide range of mixtures without being limited by chemical kinetics. However, as mentioned, the specific modes of flame propagation were observed such as cap-like flame in ultra-lean H_2/air flames [28]. These observed flame structure can affect the heat transfer mechanism during flame propagation. Thus, more studies should be performed to investigate the effects of a specific flow regime. This is also our further study.

4.2. Role of elevated temperature

The CNAFT coefficient contains several thermal properties including thermal conductivity and heat capacity. It is important to investigate which properties dominantly affect the coefficient when the individual conditions of the mixture were changed. These key property identifications make it possible to quantitively predict the change of LFL even for the more complex mixture condition changes. First, we identified the key property at the temperature increase. As shown in Fig. 8, the CNAFT coefficient of the mixtures becomes larger as the initial temperature increases. These results included temperature increases in H_2-air mixtures without diluent. The value of relative increase was calculated based on the reference mixture at room temperature as before. When the initial

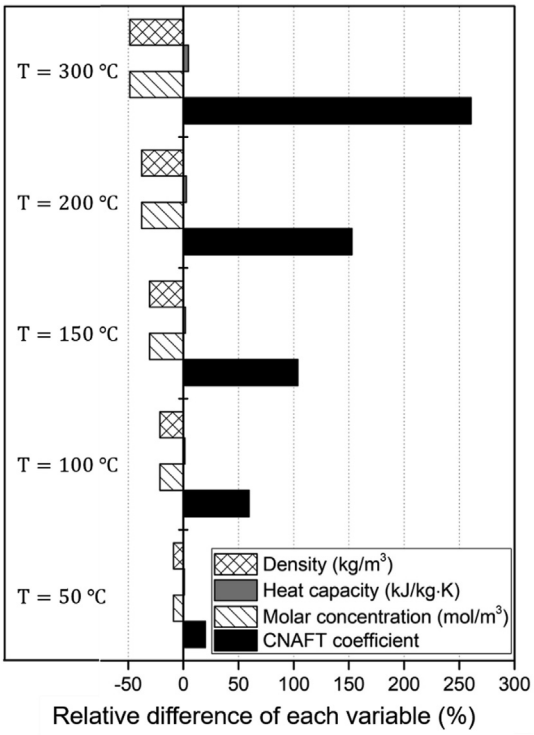

Fig. 8. Increases of the CNAFT coefficient as the initial temperature increases for H_2-air mixtures.

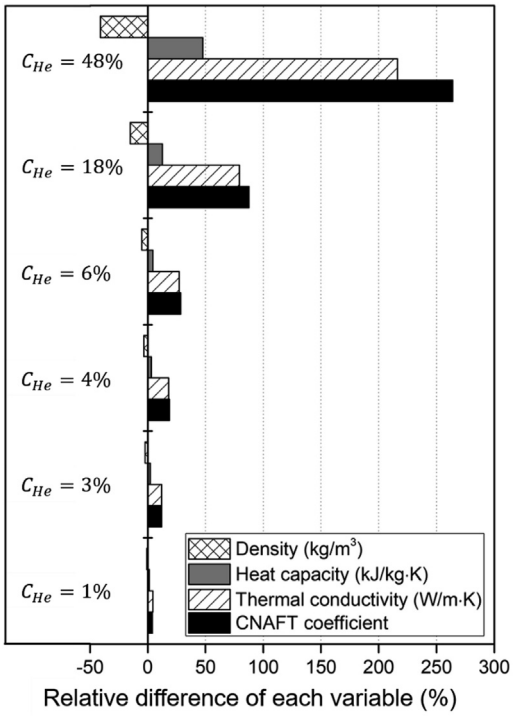

Fig. 9. Increases of the CNAFT coefficient as the helium concentration increases for H_2-air-He mixtures.

temperature increases to 300 °C, the relative increase exceeds 250% because the density and molar concentration decrease. The decrease in density of unburnt gas leads to an increase in the temperature gradient to the post reaction zone at same volumetric radiation rate. The molar concentration is also proportional to density because the average molecular weight is constant at same constituent gases. In addition, changes in heat capacity were found to be negligible when the initial mixture temperature increases. As a result, these analyses can explain why the elevation of initial temperature for hydrogen mixture always leads to an uncertainty increase for previous CAFT model.

4.3. Role of additional diluents

When the helium concentration increases to 48%, the relative increase also exceeds 250% as shown in Fig. 9. These results are based on H_2-air-He mixtures at the room temperature and the thermal conductivity is calculated at reference temperature (610 K). The reason why the CNAFT coefficient increases with helium gas is completely different to the temperature case. The addition of helium gas causes soar of heat loss magnitude because of high thermal conductivity independently of the temperature gradient to the post reaction zone. The thermal conductivity increases by over 200% based on the H_2-air-He (48%). The heat capacity also increases about 50% based on the H_2-air-He (48%). The increase of heat capacity contributes to reducing the coefficient, which determines the amount of heat loss. Generally the increase of the heat capacity with diluent concentration reducing the combustion risk cannot be applied to the heat loss calculation [36]. However, as density decreases as opposed to the heat capacity, these two variables do not effectively contribute to the variation of the CNAFT coefficient.

On the other hand, nitrogen and argon which do not contribute the increase in heat loss were also analyzed. When nitrogen is added to the mixture, the volumetric hydrogen concentration decreases and the inert effect can be obtained. However, the increase in nitrogen concentration does not increase the intrinsic LFL of hydrogen mixture itself in the experimental results [21]. The reason for that trend can be quantitatively explained by Fig. 10. These results are also based on H_2-air-N_2 at the room temperature. In conclusion, all properties included in the CNAFT coefficient did not make noticeable changes with increasing nitrogen concentration. This is as expected because most of the air is composed of nitrogen. Even in the case of argon, the CNAFT coefficient decreases with increasing concentration as shown in Fig. 11. It is because, contrary to helium, argon has a very small thermal conductivity compared to

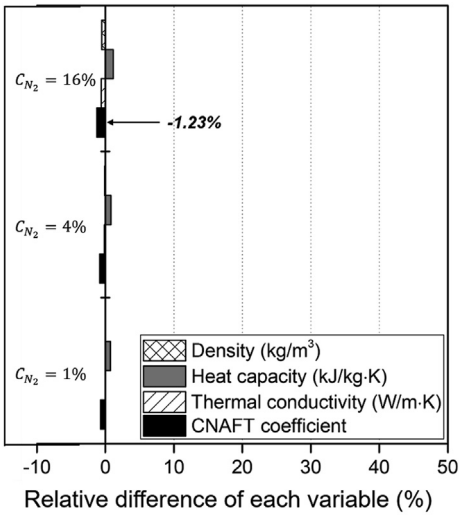

Fig. 10. Consistency of the CNAFT coefficient as the nitrogen concentration increases for H_2-air-N_2 mixtures.

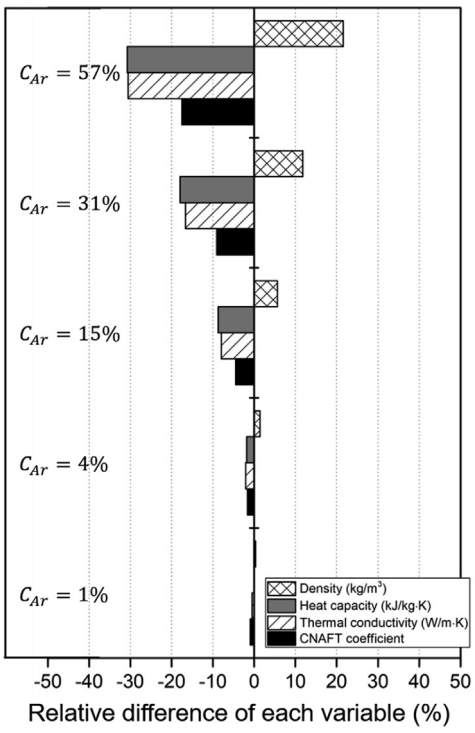

Fig. 11. Decrease of the CNAFT coefficient as the argon concentration increases for H_2-air-Ar mixtures.

air. The decrease of specific heat is affinity to the heat loss mechanism, but as the density increases, the coefficient finally decreases. The slight decrease in LFL with increasing argon concentration can be explained by these physical descriptions. As a result, these analyses of CNAFT coefficient with thermal properties provide clear understanding on changes of LFL depending on the diluent types.

5. Conclusion

In this study, a CNAFT model was developed to predict the LFL of hydrogen mixtures based on the heat transfer characteristics in flame propagation. Agreement with experimental results on H_2-air-diluent mixtures was improved significantly, especially for mixtures at an elevated initial temperature and with high helium concentrations, for which the previous model (CAFT) showed technical limitations. Consequently, we propose that this heat transfer-based model can be applicable to a wide range of hydrogen mixtures at elevated initial temperature and additional diluents without being limited by chemical kinetics. It means that the model can ultimately contribute to the thorough hydrogen risk analysis under severe accidents. Our major findings and future work can be summarized as follows.

(1) The CNAFT coefficient was derived to estimate the amount of radiative heat loss according to the mixture properties. This derivation is based on the heat loss rate from the reaction zone due to conduction into the post-reaction zone. The mixtures for which the previous model showed technical limitations yielded a higher coefficient than the other mixtures.
(2) We confirmed that the magnitude of the radiative heat loss in the CNAFT model can be estimated via the CNAFT coefficient after verification with experimental results. Mixtures having a higher coefficient require more combustion heat to compensate for their higher radiative heat loss.
(3) Only the CNAFT model, which considers the heat loss mechanism according to initial temperature and diluent concentration, exhibits reliable LFL accuracy when compared with experimental results. The model reliability was confirmed for H_2-air mixtures up to 300 °C and H_2-air-He mixtures up to 50 vol% helium concentration.
(4) The analyses of CNAFT coefficient with thermal properties provide clear understanding on changes of LFL depending on diluent types. The addition of helium gas causes soar of heat loss magnitude because of high thermal conductivity and leads to the increase of LFL. On the contrary, the slight decrease in LFL with increasing argon concentration can be explained by smaller thermal conductivity compared to air. In case of nitrogen, the LFL is insensitive to nitrogen concentration because all properties included in the CNAFT coefficient did not make noticeable changes.

Acknowledgements

This work was supported by KOREA HYDRO & NUCLEAR POWER CO., LTD (No. 2017-tech-9).

Appendix A. Supplementary data

Supplementary data to this article can be found online at https://doi.org/10.1016/j.net.2019.05.005.

References

[1] T. Nishimura, H. Hoshi, A. Hotta, Current research and development activities on fission products and hydrogen risk after the accident at Fukushima Daiichi nuclear power station, Nucl. Eng. Technol 47 (2015) 1–10.
[2] S.W. Hong, J. Kim, H.-S. Kang, Y.-S. Na, J. Song, Research efforts for the resolution of hydrogen risk, Nucl. Eng. Technol 47 (2015) 33–46.
[3] N.K. Kim, J. Jeon, W. Choi, S.J. Kim, Systematic hydrogen risk analysis of OPR1000 containment before RPV failure under station blackout scenario, Ann. Nucl. Energy 116 (2018) 429–438.
[4] S. Gupta, Experimental investigations relevant for hydrogen and fission product issues raised by the Fukushima accident, Nucl. Eng. Technol 47 (2015) 11–25.
[5] A. Bentaib, N. Meynet, A. Bleyer, Overview on hydrogen risk research and development activities: methodology and open issues, Nucl. Eng. Technol 47 (2015) 26–32.
[6] D.Y. Kim, J.H. Kim, K.H. Yoo, M.G. Na, Prediction of hydrogen concentration in containment during severe accidents using fuzzy neural network, Nucl. Eng. Technol 47 (2015) 139–147.
[7] K. Malik et al., Detonation cell size model based on deep neural network for hydrogen, methane and propane mixtures with air and oxygen, Nucl. Eng. Technol. https://doi.org/10.1016/j.net.2018.11.004.
[8] J. Yu, B. Hou, A. Lelyakin, Z. Xu, T. Jordan, Gas detonation cell width prediction model based on support vector regression, Nucl. Eng. Technol 49 (2017) 1423–1430.
[9] L.L. Humphries, R.K. Cole, D.L. Louie, V.G. Figueroa, M.F. Young, MELCOR Computer Code Manuals, Sandia National Laboratories, Albuquerque, USA, 2015. SAND2015-6692R.
[10] P. Nikolaidis, A. Poullikkas, A comparative overview of hydrogen production processes, Renew, Sustain. Energy Rev. 67 (2017) 597–611.
[11] A.L. Sánchez, F.A. Williams, Recent advances in understanding of flammability characteristics of hydrogen, Prog. Energy Combust. Sci. 41 (2014) 1–55.
[12] T. Ma, A thermal theory for estimating the flammability limits of a mixture, Fire Saf. J. 46 (2011) 558–567.
[13] D.B. Spalding, A theory of inflammability limits and flame-quenching, Proc. Roy. Soc. Lond. A 240 (1957) 83–100.
[14] M. Vidal, W. Wong, W.J. Rogers, M.S. Mannan, Evaluation of lower flammability limits of fuel–air–diluent mixtures using calculated adiabatic flame temperatures, J. Hazard Mater. 130 (2006) 21–27.
[15] M.G. Zabetakis, Flammability Characteristics of Combustible Gases and Vapors, US Bureau of Mines, Bulletin 627, Washington, 1965.
[16] T.K.H. Cheng, An Experimental Study of the Rich Flammability Limits of Some Gaseous Fuels and Their Mixtures in Air, MSc Thesis, Department of Mechanical Engineering, University of Calgary, 1985.
[17] S.O. Bade Shrestha, Systematic Approach to Calculations of Flammability Limits of Fuel-Diluent Mixtures in Air, MSc Thesis, Department of Mechanical

Engineering, University of Calgary, 1992.
[18] G. Shu, B. Long, H. Tian, H. We, X. Liang, Flame temperature theory-based model for evaluation of the flammable zones of hydrocarbon-air-CO2 mixtures, J. Hazard Mater. 294 (2015) 137–144.
[19] M. Wu, G. Shu, R. Chen, H. Tian, X. Wang, Y. Wang, A new model based on adiabatic flame temperature for evaluation of the upper flammable limit of alkane-air-CO2 mixtures, J. Hazard Mater. 344 (2018) 450–457.
[20] Y. Ju, G. Masuya, P.D. Ronney, Effects of radiative emission and absorption on the propagation and extinction of premixed gas flames, Proc. Combust. Inst. 27 (1998) 2619–2626.
[21] M. Terpstra, Flammability Limits of Hydrogen-Diluent Mixtures in Air, MSc thesis, University of Calgary, 2012.
[22] R.K. Kumar, Flammability limits of hydrogen-oxygen-diluent mixtures, J. Fire Sci. 3.4 (1985) 245–262.
[23] J.E. Hustad, O.K. Sønju, Experimental studies of lower flammability limits of gases and mixtures of gases at elevated temperatures, Combust. Flame 71 (1998) 283–294.
[24] I. Glassman, R.A. Yetter, N.G. Glumac, Combustion, Academic press, 2015.
[25] H.F. Coward, G.W. Jones, Limits of Flammability of Gases and Vapors, US Bureau of Mines, Pittsburgh, Pennsylvania, USA, 1957. Bulletin 627.
[26] E.A. Ural, R.G. Zalosh, A mathematical model for lean hydrogen-air-steam mixture combustion in closed vessel, Proc. Combust. Inst. 20 (1984) 1727–1734.
[27] E. Mayer, A theory of flame propagation limits due to heat loss, Combust. Flame 1 (1957) 438–452.
[28] Z. Zhou, Y. Shoshin, F.E. Hernandez-Perez, et al., Experimental and numerical study of cap-like lean limit flames in H_2-CH_4-air mixtures, Combust. Flame 189 (2018) 212–224.
[29] D. Fernandez-Galisteo, A.L. Sanchez, A. Linan, F.A. Williams, The hydrogen-air burning rate near the lean flammability limit, Combust. Theor. Model 13 (2009) 741–761.
[30] H.J. Liaw, K.Y. Chen, A model for predicting temperature effect on flammability limits, Fuel 178 (2016) 179–187.
[31] K.P. Lakshmisha, P. Paul, H. Mukunda, On the flammability limit and heat loss in flames with detailed chemistry, Proc. Combust. Inst. 23 (1991) 433–440.
[32] Y. Shoshin, J. Jarosinski, On extinction mechanism of lean limit methane-air flame in a standard flammability tube, Proc. Combust. Inst. 32 (2009) 1043–1050.
[33] Y. Dong, A.T. Holley, M.G. Andac, et al., Extinction of premixed H_2/air flames: chemical kinetics and molecular diffusion effect, Combust. Flame 142 (2005) 374–387.
[34] R.M. Davies, G. Taylor, The mechanics of large bubbles rising through extended liquids and through liquids in tubes, Proc. R. Soc. A. Math. Phys. Eng. Sci. 200 375–390.
[35] A. Levy, An optical study of flacmmability limits, Proc. Roy. Soc. Lond. A 283 (1965) 134–145.
[36] B. Zhang, G. Xiu, C. Bai, Explosion characteristics of argon/nitrogen diluted natural gas-air mixtures, Fuel 124 (2014) 125–132.